Cranked Hartree-Fock-Bogoliubov calculations in the Xe-Ba region

M. Saha Sarkar
Saha Institute of Nuclear Physics, 1/AF Bidhan Nagar, Calcutta 700064, India

S. Sen*
Department of Science, Technology & NES, Government of West Bengal, Bikash Bhavan, Calcutta 700091, India

(Received 31 July 1997)

Properties of the ground state and first 2^+ state of a large number of even-even nuclei in the Xe-Ba region have been calculated using a simple version of cranked Hartree-Fock-Bogoliubov model. The parameter set used has been obtained by fitting the ground state properties of some of the nuclei in this region. The sensitivity of the results to the choice of parameters has also been tested in a few cases. The shape rigidity of the nuclei in this mass region has been studied by generating energy contours in the β_2-γ plane. Influence of the hexadecapole deformation on nuclei having flat energy surfaces in the γ direction has been examined. Higher angular momentum states also (up to 6^+ or 10^+) have been calculated in some of the nuclei to study the evolution of shape and nature of alignment with increasing spin. [S0556-2813(97)06111-6]

PACS number(s): 21.60.Ev, 21.60.Cs, 21.60.Jz, 27.60.+j

I. INTRODUCTION

The study of nuclear structure [1,2] of the isotopes of tellurium to cerium nuclei has provided us with a wealth of information on both collective and particle excitations.

There exists an exhaustive list of theoretical as well as experimental investigations devoted to the study of the structure of this complex transitional region [1–5]. This is the heaviest mass region where proton and neutron excitations within the same major shell can compete. There are two important consequences of this competition. First, unlike in the rare earth region, where particles responsible for the first backbending in the even-even nuclei are always neutrons, in the Xe-Ba region there are evidences of two parallel superbands corresponding to the neutron and proton alignments (forking of band). So in this region it may be neutrons or protons which cause the first backbending depending upon the particular isotope concerned. Secondly, potential-energy surface (PES) and cranked-shell model (CSM) calculations suggest that these high-j valence particles exert a strong and specific deformation driving force on the γ-soft core; particles in the lower part of the $h_{11/2}$ subshell favor a collectively rotating prolate shape ($\gamma \simeq 0°$) in the Lund convention [6], while those in the $h_{11/2}$ upper midshell favor a collectively rotating oblate shape ($\gamma \simeq -60°$).

This is a region where one can study the variation of shape from spherical to well deformed through triaxial within a isotopic series (increasing N, same Z) or within a chain of isotones (same N, increasing Z). Similarly, the nature of band crossing, i.e., whether they are due to proton or neutron alignment is not always established beyond doubt. In fact, the most sensitive physical variables, i.e., magnetic moments of high spin states which can be used as a very good probe to study the nature of alignment, have been measured only in a very few cases in this mass region. So though many theoretical and experimental investigations have been done in this region, there are still several open questions which can be addressed through further investigations.

In the cranked Hartree-Fock-Bogoliubov (CHFB) formalism, the potential parameters are determined self-consistently. In spite of its several shortcomings, this formalism has been used extensively to investigate the complexity of the nuclear excitation spectra, arising from the interplay of single-particle and collective aspects of nuclear motion, as a function of rotational frequency. To have a microscopic view of the variation of shape, pairing gaps, and g factors with spin, mass, and atomic numbers for the nuclei in the Xe-Ba transitional region, self-consistent CHFB calculations with the pairing-plus-quadrupole (PPQ) Hamiltonian of Baranger and Kumar (BK) [7] have been performed.

The CHFB formalism using PPQ Hamiltonian has been widely used in the rare earth region to study the variation of g factor, deformation, and pairing gap with spins [8–10]. The parameters (including the set of spherical single particle energies) used in these calculations are mostly chosen according to the suggestions of Baranger and Kumar from their exhaustive study [7] of the ground state properties of these nuclei. A few attempts [9,10] were also made to have a better set of parameters. There is no such exhaustive study in this region. But proper choice of parameter is the primary requirement to study a specific region with a particular model. In this work we have tried to get a reasonable set of parameters for this region and study various aspects of nuclear structure using the above model. The main purpose of our study is not to fit any experimental data, backbending, or g factors, whatsoever, in a particular isotope very accurately. But we want to understand, as far as possible, the applicability of this model, in its usual form, in this transitional region and to study the gross features of the nuclear structure of this region. We have not, therefore, made any adjustment of the strengths of the residual interactions from isotope to isotope (except for a few special cases), although we have studied a wide mass region from $A=122$ to 148.

With this in view, we have obtained a set of parameters

*On leave from Saha Institute of Nuclear Physics, 1/AF Bidhan Nagar, Calcutta 700064, India.

by fitting the experimental data (e.g., ground state deformation and pairing gaps, excitation energies, nature of aligning particles, and g factors of the ground state band from 0^+ to 10^+, wherever available) in ^{122,124}Xe and ^{126}Ce. Next we have calculated the 0^+ and 2^+ states of $^{120-122}$Te, $^{126-132}$Xe, $^{130-136}$Ba, $^{142-146}$Ba with this set of parameters. For ^{132}Ba, calculations have been done for the 10^+ state also to check whether this set of parameters can reproduce the g factor of this state measured recently [11]. For the ^{132,134,146,148}Ce isotopes, properties of the states from 0^+ to 6^+ have been calculated. We have also tested the sensitivity of the results with respect to the change of parameters in a few cases. The shape rigidity of the nuclei in this mass region has been studied by generating energy contours in the β_2-γ plane. Influence of the hexadecapole deformation on nuclei having flat energy surfaces in the γ direction has also been examined.

Since the model used in this work is well known, only some of its relevant features are presented here. Results of the calculation are discussed in detail in subsequent sections keeping in view the objectives of the present work.

II. CHFB FORMALISM

A. Model

In the cranking model, the Hamiltonian H_ω is cranked about an axis (here, x axis) perpendicular to the symmetry axis (here, z axis) of the nucleus

$$H_\omega = H - \omega \hat{I}_x - \lambda \hat{N}, \tag{1}$$

where ω is the Lagrange multiplier (given in energy units, interpreted as the cranking frequency for rotation about x axis) such that total angular momentum of the system is given by the constraint,

$$I_x = \langle \psi_{\mathrm{CHFB}}(\omega) | \hat{I}_x | \psi_{\mathrm{CHFB}}(\omega) \rangle = \sqrt{I(I+1)} \tag{2}$$

along with the usual constraint on the particle number N, due to the presence of pairing interaction term in the Hamiltonian H. Here λ, interpreted as the Fermi level, is the Lagrange multiplier used to ensure the conservation of ''average'' particle number,

$$\langle \psi_{\mathrm{CHFB}}(\omega) | \hat{N}_\tau | \psi_{\mathrm{CHFB}}(\omega) \rangle = N_\tau, \tag{3}$$

where N_τ denotes proton or neutron number outside the core. For compensating small numerical errors in satisfying the above relation we have added a correction term in the energy E [10,12].

In Eq. (1), H is given by a more general form (to include the hexadecapole term) of the pairing plus quadrupole model Hamiltonian of Baranger and Kumar [7]:

$$\begin{aligned} H = & \sum_{a\tau} \varepsilon_{a\tau} C_a^\dagger C_a - \frac{1}{2} \sum_{\lambda=2,4} \sum_{abcd\mu\tau\tau'} \alpha_\tau \alpha_{\tau'} \langle a | Q_{\lambda\mu}^\tau | c \rangle \\ & \times \langle b | (-1)^\mu Q_{\lambda-\mu}^{\tau'} | d \rangle C_a^\dagger C_b^\dagger C_d C_c \\ & - \frac{1}{4} \sum_\tau G_\tau \sum_{ac} C_a^\dagger C_{\bar{a}}^\dagger C_{\bar{c}} C_c . \end{aligned} \tag{4}$$

Here $|a\rangle$, $|b\rangle$, . . . are the symmetrized signature basis states [13]. Various symbols have their usual meanings; τ, τ' being neutron or proton. In general,

$$Q_{\lambda\mu} = r^2 Y_{\lambda\mu}(\theta, \phi) \tag{5}$$

and β_2 and γ are given by

$$\hbar\omega_o \beta_2 \cos\gamma = D_{20}, \quad \hbar\omega_o \beta_2 \sin\gamma = \sqrt{2} D_{22}, \tag{6}$$

where

$$D_{2\mu} = \chi_2 \sum_\tau \alpha_\tau \langle Q_{2\mu} \rangle_\tau = (-1)^\mu D_{2-\mu} \tag{7}$$

and [10,14]

$$D_{4\mu} = \chi_4 \sum_\tau \alpha_\tau \langle Q_{4\mu} \rangle_\tau = (-1)^\mu D_{4-\mu} . \tag{8}$$

We have defined β_4 through the relation

$$\hbar\omega_o \beta_4 = D_{40} . \tag{9}$$

The radial coordinate is given in units of oscillator length

$$\tilde{b} = (\hbar / m\omega_o)^{1/2}, \tag{10}$$

which is connected with the oscillator energy

$$\hbar\omega_o = 41.2 A^{1/3} \ \mathrm{MeV}. \tag{11}$$

The parameters

$$\alpha_\tau = \begin{cases} (2Z/A)^{1/3} & \text{for protons,} \\ (2N/A)^{1/3} & \text{for neutrons} \end{cases} \tag{12}$$

have been introduced by Baranger and Kumar to ensure equal radii for protons and neutrons.

The g factors are calculated from $\hat{\mu}_x$, x is the component of magnetic moment operator $\hat{\mu}$, as

$$g_I = \langle \psi_{\mathrm{CHFB}} | \hat{\mu}_x | \psi_{\mathrm{CHFB}} \rangle / I_x . \tag{13}$$

We have attenuated the values of $(g_s)_{\mathrm{free}}$ (spin g factor) by 0.6. So

$$g_I = [\langle \hat{I}_x^p \rangle + 2.351 (\langle \hat{s}_x^p \rangle - 0.98 \langle \hat{s}_x^n \rangle)] / \sqrt{I(I+1)}. \tag{14}$$

Besides this, we have generated energy contour plots of some nuclei in the β_2-γ plane corresponding to each β_2, γ mesh point. Pairing gaps (Δ_p and Δ_n) have been determined self-consistently for each of the mesh points. For contour plots including hexadecapole degree of freedom, we have considered a fixed value of β_4 and determined the self-consistent minimum.

B. Parameter choice

The oscillator shells $N=4$ and 5 are included in the basis states for both protons and neutrons for nuclei with mass number $A \leqslant 140$. For nuclei with higher masses, we have used the oscillator shells $N=5$ and 6 for neutrons. The inert cores are, therefore, $^{80}_{40}\mathrm{Zr}_{40}$, $^{110}_{40}\mathrm{Zr}_{70}$, respectively. Zhang *et al.* [15] have suggested single particle parameter sets

TABLE I. Different parameter sets used in the present calculations.

Set	s.p.e. [a]	G_p	G_n	χ_2	Comments
A	Zhang	28.0	24.0	78.0	General set — reproduces average behaviour
B	Zhang	26.0	24.0	78.0	$N=76$, best for $^{132}_{56}$B
C	Nil	28.0	24.0	78.0	-
D	Zhang	26.0	22.0	78.0	$N=74$, best for $^{130}_{56}$Ba
E	Zhang	26.0	24.0	75.0	for $^{142-146}_{56}$Ba
F	Nil	26.0	24.0	75.0	for $^{142-146}_{56}$Ba
G	Zhang	28.0	24.0	75.0	for $^{142-148}_{56}$Ba

[a]Single particle energies: Zhang from Ref. [15] and Nil from Ref. [16].

(μ, κ values) for proton shells $N=4$, 5, and 6 for $A\approx 120-140$ regions by searching for the best theoretical fit to the experimental bandhead energies. Using their μ, κ values, they achieved a significant improvement in the theoretical fit to the available bandhead energies in odd-proton nuclei over the entire $A\approx 120-140$ region. These fits, which were made over a region defined by $53\leqslant Z\leqslant 63$ and $64\leqslant N\leqslant 80$, included 28 bandhead energies. The parameter sets suggested for the neutrons are more or less the same as suggested by Nilsson *et al.* [16]. We have used the parameter set suggested by Zhang to obtain spherical single particle energies.

Baranger and Kumar (BK) [7] did an extensive work to choose the parameters of the pairing-plus-quadrupole model as realistically as possible in the mass region $A=138-208$ with $Z=56-82$. But we have not come across any such study for the mass region $A=120-140$ with $Z=52-58$. BK have suggested some closed expressions for the quadrupole force strength as a function of mass number, which should give ''an excellent description of the overall variation of χ across many shells,'' but ''the variation inside each individual shell can be expected to be considerably slower than this.'' Their final suggestion is to determine the force strength by fitting the data. Regarding the choice of pairing force strength, they could not suggest any reliable way of predicting the strengths as they did for quadrupole force strengths. But in their calculations the values of G_p and G_n were determined by fitting the proton and neutron odd-even mass differences.

We have determined the proton and neutron pairing (G_p, G_n) and quadrupole deformation strength (χ_2) parameters by reproducing the ground state band properties of a few nuclei in this region (see set A in Table I). We have considered the following points for choosing a reasonable set of parameters.

(i) Previous calculations suggest that the first band crossing in the yrast spectra of ^{122,124}Xe is due to the alignment of a pair of neutrons in the $h_{11/2}$ orbitals. The same is reproduced in the CHFB calculation.

(ii) We have tried to reproduce quite accurately the experimental energies of the yrast band of these nuclei, namely, ^{122,124}Xe and ^{126}Ce.

(iii) The magnetic moments have been measured for the $I^+=10^+$ and 12^+ states of a close lying (with respect to the ground band) sideband in ^{126}Ce [17]. This sideband originates at a spin value of 10^+. From the measured g factors, this band has been identified as a two quasiproton band of $\pi h_{11/2}$ protons. From the difference in energies between a yrast and yrare state of same spin it is expected that this sideband will cross the ground band and will be the yrast one at a spin value of $\simeq 18^+$. So unlike the Xe nuclei considered in the present work, this isotope of Ce should show a proton band crossing. We have tried to reproduce this feature.

With all these constraints, the parameter sets listed below are chosen. The pairing and quadrupole force constants are given by

$$G_p=28/A \text{ MeV}, \quad G_n=24/A \text{ MeV}, \quad \chi_2=78A^{-1.4} \text{ MeV},$$

$$\text{and } \chi_4=74A^{-1.4} \text{ MeV (chosen rather arbitrarily)}.$$

We have not included the hexadecapole term in our calculations, except for generating the energy surfaces for the ^{134}Ce isotope, which will be discussed later in detail. We have not made any adjustment of the strengths of the residual interactions (G_p, G_n, χ_2) from Te to Ce, except for some neutron numbers, which will be specified later (Table I).

III. RESULTS

The calculated yrast spectra of the ^{122}Xe, ^{124}Xe [3], and ^{126}Ce nuclei and the variation of deformation, pairing gap, g factor, etc. with spin are listed in Table II. The experimental g factors are taken from the compilation of Raghavan [17].

The results for other isotopes where only 0^+ and 2^+ states are calculated are tabulated in Table III. The results show that though there is a overall agreement with the general trend of experimental deformations, g factors, E_2^+ energies, and pairing gaps, exact agreement with the experimental numbers is sometimes missing, especially for isotopes having smaller deformations. This feature is not very unusual whenever the same parameter set is used over a wide region [10]. The ratios g_I/g_2, instead of the absolute value, g_I, were compared with experimental data in an earlier calculation [10]. The excitation energies also were deduced by normalizing the calculated E_2^+ energies with the experimental ones.

For isotopes of Ce, the results for yrast states from 0^+ to 6^+ are shown in Table IV.

We will discuss separately the results for the three isotopes, ^{122,124}Xe and ^{126}Ce in the first subsection. In the following subsections the results for the different isotopic chains will be discussed one by one.

A. $^{122,124}_{54}$Xe and $^{126}_{58}$Ce

(i) Some detailed features of the experimental data, e.g., the backbend observed in ^{124}Xe is much sharper than that observed in ^{122}Xe, are reproduced in the CHFB calculation (Table II).

(ii) In ^{124}Xe the β_2 deformation increases from ≈ 0.23 (at 0^+) to ≈ 0.25 (at $I^\pi=4^+$), then starts decreasing and reaches a value of ≈ 0.21 at $I^\pi=10^+$. For ^{126}Ce it shows a steady increase (from 0.32 at 0^+ to 0.34 at 6^+), a region of stability (0.34 from 6^+ to 10^+) and slight decrease at 12^+ to 0.33. For ^{122}Xe, β_2 increases from 0.27 to 0.30 from 0^+ to 6^+, then stabilizes at a smaller value of 0.29. This shows that ^{124}Xe is comparatively softer with respect to the β_2 value

TABLE II. Results of CHFB calculations for ^{122,124}Xe and ^{126}Ce obtained with parameter set A, Table I. Energy $E(I)$, angular frequency ω, and pairing gaps Δ_p and Δ_n are all quoted in MeV. Triaxiality parameter γ is in degrees.

		$E(I)$		Calculated						
Isotope	I	Calc.	Expt. [a]	ω	β_2	γ	Δ_p	Δ_n	g_I	g_I/g_2
$^{122}_{54}$Xe	0	0.0	0.0	0.0	0.27	0.0	1.298	1.371	-	-
	2	0.320	0.331	0.239	0.28	0.74	1.272	1.293	0.31	1.00
	4	0.908	0.828	0.330	0.29	1.28	1.244	1.154	0.24	0.78
	6	1.605	1.467	0.361	0.30	1.51	1.231	1.013	0.16	0.51
	8	2.344	2.217	0.377	0.29	1.74	1.223	0.889	0.09	0.29
	10	3.098	3.039	0.394	0.29	2.13	1.213	0.796	0.05	0.16
^{124}Xe	0	0.0	0.0	0.0	0.23	0.0	1.271	1.448	-	-
	2	0.396	0.354	0.286	0.25	1.52	1.216	1.353	0.35	1.00
	4	1.090	0.879	0.380	0.26	2.66	1.163	1.238	0.29	0.81
	6	1.879	1.549	0.385	0.24	3.97	1.153	1.162	0.14	0.41
	8	2.668	2.331	0.368	0.23	5.89	1.168	1.103	0.04	0.10
	10	3.327	3.172	0.344	0.21	10.22	1.197	1.072	-0.03	-0.09
$^{126}_{58}$Ce	0	0.0	0.0	0.0	0.32	0.0	1.446	1.175	-	-
	2	0.236	0.170	0.183	0.32	0.31	1.417	1.126	0.34	1.00
	4	0.711	0.519	0.278	0.33	0.69	1.364	1.037	0.33	0.97
	6	1.317	1.015	0.320	0.34	0.84	1.281	0.960	0.39	1.15
	8	1.956	1.625	0.305	0.34	0.41	1.091	0.987	0.65	1.91
	10	2.537	2.313	0.275	0.34	-0.27	0.848	1.032	0.83	2.44
	12	3.084	2.991	0.281	0.33	-0.94	0.629	1.028	0.88	2.59

[a]Experimental energies are taken from [23–25].

compared to the other nuclei considered (Table II).

(iii) The nucleus ^{124}Xe is significantly γ soft, i.e., the nonaxial deformation varies rapidly with spin. In this nucleus, the γ value increases from 0° (at 0^+) to 10° (at 10^+), whereas for ^{122}Xe it varies from 0° to 2° in the same spin range. In ^{126}Ce γ increases from 0° to 0.84° at spin 6^+, and then starts decreasing to $-0.94°$ at 12^+, signifying non-collective type of excitation.

(iv) This feature of the excitation mechanism in ^{126}Ce as evidenced through the negative γ value is also confirmed from the sudden large increase in the g-factor value from 0.39 (at 6^+) to 0.88 (at 12^+) in this spin range. In ^{122,124}Xe, the g factors decrease sharply indicating neutron alignment, whereas, for ^{126}Ce, sharp increase in these values indicates proton alignment.

(v) Though ^{126}Ce shows proton alignment with increasing spin as expected from the experimental data, the calculations predict a proton band crossing for this nucleus near $I^\pi = 8^+$, much earlier than the experimental trend. But this feature is not totally unexpected in a CHFB calculation using monopole pairing plus quadrupole interaction. It has been already pointed out by previous workers [18] that inclusion of only a monopole pairing term in the PPQ Hamiltonian may be partially responsible for the early backbending.

B. $^{120,122}_{52}$Te$_{68,70}$

Tellurium isotopes have only two protons above $N=50$ proton shell closure. So they are expected to show deviation from collective behavior earlier (with respect to the number of neutrons, as it approaches $N=82$ shell closure) than the neighboring nuclei ($_{54}$Xe, $_{56}$Ba, or $_{58}$Ce). The results show a reasonable agreement with the experimental data. But the decreasing trend in the 2^+ state g-factor value from the $N=68$ to $N=70$ isotope is not reproduced theoretically.

C. $^{122-132}_{54}$Xe$_{68-78}$

Experimental data available in these nuclei show that ground state quadrupole deformation decreases with neutron number from $N=70$ to 76. For $N=68$, the deformation is smaller than $N=70$. The $N=68$, ^{122}Xe isotope has a deformation of 0.231(10) [19], with $R_4(=E_4/E_2)$, $=2.50$ which is also a good indicator of collectivity. But the measured deformation of the $N=70$, ^{124}Xe isotope is 0.264(8), with the R_4 value $=2.48$. We have considered the R_4 data to be more reliable and thus expect ^{122}Xe to have same order of deformation as ^{124}Xe.

All these nuclei, except ^{122}Xe, have their 2_1^+ state g factor measured, and the experimental values show an increasing trend with increasing neutron number. The calculated results are compared with their corresponding experimental values in Table III. The systematics of theoretical g factors in $^{122-128}$Xe shows an increasing trend similar to the experimental one. Absolute values agree within the experimental error except for that in ^{124}Xe. The deformations and pairing gaps also agree reasonably. The self-consistently determined ground state deformation of ^{128}Xe comes out to be significantly smaller than its corresponding experimental value. But unlike the other two isotopes, the deformation increases for the 2^+ state and $\beta_2(2^+)$ agrees reasonably well with

TABLE III. Results of CHFB calculations for different isotopes of Te, Xe, and Ba isotopes for $I^{\pi}=0^{+}$ and 2^{+} states with various choices of parameters. Numbers quoted in squared brackets [ ] are experimental values with errors quoted in parentheses ( ). In the column for $E(I)$, the energies are with respect to the 0^{+} state. The absolute value of the energy of 0^{+} state is quoted within brackets in MeV. See also the caption of Table II.

Nucl.	Parameter set	I	ω	$E(I)$	β_2	γ	Δ_p	Δ_n	g_I
$^{120}_{52}$Te	A	0	0.0	0.0(-192.525)	0.221	0.0	1.166	1.564	-
					[0.202(21)]		[1.277]	[1.427]	
		2	0.276	0.406	0.252	1.089	1.112	1.441	0.40
				[0.560]					[+0.39(7)]
^{122}Te	A	0	0.0	0.0(-191.515)	0.115	0.0	1.158	1.751	-
					[0.1848(8)]		[1.330]	[1.378]	
		2	0.353	0.720	0.190	3.483	0.989	1.535	0.45
				[0.564]					[+0.33(2)]
$^{122}_{54}$Xe	A	0	0.0	0.0(-200.504)	0.274	0.0	1.298	1.371	-
					[0.231(10)]		[1.540]	[1.479]	
		2	0.239	0.320	0.284	0.738	1.272	1.293	0.31
				[0.331]					[-]
^{124}Xe	A	0	0.0	0.0(-198.954)	0.230	0.0	1.271	1.448	-
					[0.264(8)]		[1.344]	[1.386]	
		2	0.286	0.395	0.246	1.523	1.215	1.354	0.35
				[0.354]					[+0.23(2)]
^{126}Xe	A	0	0.0	0.0(-196.757)	0.202	0.0	1.247	1.420	-
					[0.1881(30)]		[1.311]	[1.313]	
		2	0.332	0.462	0.205	4.427	1.184	1.374	0.40
				[0.389]					[+0.37(7)]
^{128}Xe	A	0	0.0	0.0(-194.129)	0.127	0.0	1.363	1.504	-
	crude				[0.1837(49)]		[1.328]	[1.269]	
	limit	2	0.340	0.676	0.180	4.460	1.155	1.304	0.40
				[0.443]					[+0.41(7)]
^{128}Xe	A	0	0.0	0.0(-194.135)	0.114	0.0	1.390	1.535	-
	finer				[0.1837(49)]		[1.328]	[1.269]	
	limit	2	0.336	0.647	0.147	24.91	1.297	1.380	0.14
				[0.443]					[+0.41(7)]
^{130}Xe	A	0	0.0	0.0(-191.231)	0.034	0.0	1.445	1.513	-
					[0.169(6)]		[1.260]	[1.513]	
		2	0.338	0.905	0.106	21.905	1.344	1.194	-0.02
				[0.538]					[+0.38(7)]
^{132}Xe	A	0	0.0	0.0(-187.901)	0.010	0.0	1.421	1.326	-
					[0.1409(46)]		[1.190]	[1.202]	
^{130}Xe	B	0	0.0	0.0(-190.575)	0.030	0.0	1.276	1.517	-
					[0.169(6)]		[1.260]	[1.513]	
^{124}Xe	C	0	0.0	0.0(-220.301)	0.227	0.0	1.395	1.427	-
					[0.264(8)]		[1.344]	[1.386]	
		2	0.299	0.423	0.245	1.511	1.353	1.325	0.30
				[0.354]					[+0.23(2)]

TABLE III. *(Continued).*

Nucl.	Parameter set	I	ω	$E(I)$	β_2	γ	Δ_p	Δ_n	g_I
^{126}Xe	C	0	0.0	0.0(-218.312)	0.170	0.0	1.413	1.472	-
					[0.1881(30)]		[1.311]	[1.313]	
		2	0.372	0.588	0.193	5.627	1.328	1.350	0.30
				[0.389]					[+0.37(7)]
$^{130}_{56}$Ba	A	0	0.0	0.0(-200.161)	0.179	0.0	1.413	1.351	-
					[0.230(12)]		[1.346]	[1.338]	
		2	0.340	0.506	0.193	7.117	1.334	1.251	0.32
				[0.357]					[+0.35(3)]
^{132}Ba	A	0	0.0	0.0(-196.816)	0.101	0.0	1.545	1.390	-
					[0.186(6)]		[1.358]	[1.231]	
		2	0.331	0.808	0.135	26.549	1.470	1.212	0.04
				[0.465]					[+0.34(3)]
^{134}Ba	A	0	0.0	0.0(-193.442)	0.019	0.0	1.601	1.291	-
					[-]		[1.313]	[1.195]	
^{136}Ba	A	0	0.0	0.0(-189.576)	0.005	0.0	1.571	0.984	-
					[-]		[1.180]	[1.085]	
^{142}Ba	A	0	0.0	0.0(-239.353)	0.025	0.0	1.469	1.354	-
					[0.157(6)]		[1.218]	[0.906]	
		2	0.378	1.046	0.082	-3.503	1.402	1.182	0.037
				[0.359]					[+0.426(48)]
^{144}Ba	A	0	0.0	0.0(-249.458)	0.210	0.0	1.094	1.298	-
					[0.193(6)]		[1.202]	[0.815]	
		2	0.223	0.345	0.238	0.369	1.004	1.244	0.38
				[0.199]					[+0.34(5)]
^{146}Ba	A	0	0.0	0.0(-261.073)	0.373	0.0	0.986	0.921	-
					[0.218(8)]		[-]	[-]	
		2	0.079	0.081	0.392	0.026	0.962	0.806	0.22
				[0.181]					[+0.28(7)]
^{130}Ba	B	0	0.0	0.0(-199.562)	0.182	0.0	1.183	1.356	-
					[0.230(12)]		[1.346]	[1.338]	
		2	0.295	0.427	0.199	9.878	1.078	1.265	0.44
				[0.357]					[+0.35(3)]
^{132}Ba	B	0	0.0	0.0(-196.072)	0.114	0.0	1.322	1.377	-
					[0.186(6)]		[1.358]	[1.231]	
		2	0.337	0.550	0.151	24.378	1.202	1.210	0.31
				[0.465]					[+0.34(3)]
^{142}Ba	B	0	0.0	0.0(-238.600)	0.0315	0.0	1.293	1.351	-
					[0.157(6)]		[1.218]	[0.906]	
		2	0.363	0.926	0.124	3.663	1.088	1.149	0.286
				[0.359]					[+0.426(48)]
^{144}Ba	B	0	0.0	0.0(-249.058)	0.199	0.0	0.924	1.318	-
					[0.193(6)]		[1.202]	[0.815]	
		2	0.165	0.246	0.268	0.265	0.731	1.221	0.42
				[0.199]					[+0.34(5)]

TABLE III. *(Continued).*

Nucl.	Parameter set	I	ω	$E(I)$	β_2	γ	Δ_p	Δ_n	g_I
^{146}Ba	B	0	0.0	0.0(-260.744)	0.370 [0.218(8)]	0.0	0.808 [-]	0.936 [-]	-
		2	0.074	0.057 [0.181]	0.394	0.026	0.791	0.805	0.28 [+0.28(7)]
^{130}Ba	D	0	0.0	0.0(-198.868)	0.196 [0.230(12)]	0.0	1.146 [1.346]	1.046 [1.338]	-
		2	0.247	0.345 [0.357]	0.205	3.651	1.074	0.957	0.32 [+0.35(3)]
^{132}Ba	D	0	0.0	0.0(-195.341)	0.139 [0.186(6)]	0.0	1.262 [1.358]	1.086 [1.231]	-
		2	0.282	0.391 [0.465]	0.166	20.884	1.164	0.917	0.29 [+0.34(3)]
^{142}Ba	D	0	0.0	0.0(-237.738)	0.0748 [0.157(6)]	0.0	1.243 [1.218]	1.107 [0.906]	-
		2	0.292	0.626 [0.359]	0.135	3.508	1.080	0.909	0.223 [+0.426(48)]
^{142}Ba	E	0	0.0	0.0(-238.592)	0.0266 [0.157(6)]	0.0	1.295 [1.218]	1.352 [0.906]	-
		2	0.363	1.022 [0.359]	0.115	3.798	1.091	1.150	0.316 [+0.426(48)]
^{144}Ba	E	0	0.0	0.0(-248.511)	0.163 [0.193(6)]	0.0	1.004 [1.202]	1.357 [0.815]	-
		2	0.275	0.421 [0.199]	0.183	1.524	0.867	1.291	0.54 [+0.34(5)]
^{146}Ba	E	0	0.0	0.0(-258.921)	0.285 [0.218(8)]	0.0	0.728 [-]	1.239 [-]	-
		2	0.152	0.162 [0.181]	0.271	0.224	0.697	1.264	0.41 [+0.28(7)]
^{144}Ba	F	0	0.0	0.0(-258.637)	0.159 [0.193(6)]	0.0	1.134 [1.202]	1.432 [0.815]	-
		2	0.273	0.472 [0.199]	0.202	1.712	1.003	1.335	0.44 [+0.34(5)]
^{146}Ba	F	0	0.0	0.0(-269.361)	0.367 [0.218(8)]	0.0	0.904 [-]	0.927 [-]	-
		2	0.083	0.104 [0.181]	0.368	0.051	0.897	0.903	0.28 [+0.28(7)]

experimental ground state deformation $\beta_2(0^+)$. The corresponding value of $\gamma(2^+)$ is small ($\simeq 4°$). For crude limits of iteration this configuration comes out as a minimum energy configuration, with angular momentum value at 2.30 instead of 2.44. The g-factor value for the 2^+ state ($\simeq 0.40$) also agrees with experiment ($\simeq 0.41$) quite reasonably for this limit. But in the finer limit of iteration, the energy is minimized for a triaxial shape with γ value $\approx 25°$ with a gain of 6 keV energy compared to the minimum at $\gamma = 0°$. The g-factor value ($\simeq 0.14$) also deviates largely from the experimental number. The theoretical 2^+ state energies [20], for these three isotopes are systematically larger than the experimental values.

The change in the ground state structure of these nuclei with neutron number is clearly seen in the energy contour plots for ^{124}Xe and ^{128}Xe nuclei in Figs. 1 and 2. For ^{124}Xe, there is single distinct prolate minimum along the β_2 axis at a value of $\simeq 0.26$ with γ value $\simeq 0.0$. The energy contours for ^{128}Xe on the other hand are essentially γ independent, which in effect predicts a γ-soft behavior for this nucleus.

TABLE IV. Results for various isotopes of Ce for $I^{\pi} = 0^{+}$ to 6^{+}. Also see the captions of the previous tables.

Nucl.	Parameter set	I	ω	$E(I)$	β_2	γ	Δ_p	Δ_n	g_I
$^{132}_{58}$Ce	A	0	0.0	0.0(-205.316)	0.198	0.0	1.503	1.279	-
					[0.257(10)]		[1.316]	[1.140]	
		2	0.321	0.465	0.208	4.817	1.453	1.191	0.31
				[0.325]					
		4	0.359	1.161	0.212	10.15	1.435	1.055	0.16
		6	0.338	1.863	0.204	17.27	1.467	0.934	0.02
^{134}Ce	A	0 [a]	0.0	0.0(-201.743)	0.134	1.375	1.596	1.298	-
					[0.194(8)]		[1.363]	[1.171]	
		0 [a]	0.0	0.0	0.133	0.0	1.597	1.299	-
		2 [b]	0.342	0.587	0.165	20.44	1.529	1.137	0.20
				[0.409]					
		2 [b]	0.382	0.730	0.157	2.302	1.521	1.166	0.15
		4	0.309	1.216	0.148	30.02	1.574	1.046	-0.04
		6	0.223	1.673	0.124	64.21	1.653	1.027	-0.17
^{146}Ce	A	0	0.0	0.0(-254.321)	0.322	0.0	1.082	1.046	-
					[0.174(12)]		[1.178]	[1.056]	
		2	0.120	0.155	0.324	0.147	1.070	1.020	0.28
				[0.258]					[+0.24(5)]
		4	0.176	0.459	0.334	0.327	1.034	0.925	0.25
		6	0.190	0.827	0.339	0.329	1.018	0.807	0.17
^{148}Ce	A		0.0	0.0(-266.399)	0.394	0.0	0.988	0.816	-
					[0.246(10)]		[1.102]	[0.795]	
		2	0.075	0.088	0.397	0.020	0.975	0.779	0.25
				[0.159]					[+0.37(6)]
		4	0.119	0.270	0.409	0.052	0.932	0.687	0.25
		6	0.154	0.545	0.410	0.087	0.909	0.608	0.23
^{146}Ce	G	0	0.0	0.0(-253.604)	0.164	0.0	1.322	1.324	-
					[0.174(12)]		[1.178]	[1.056]	
		2	0.309	0.501	0.188	2.003	1.246	1.230	0.33
				[0.258]					[+0.24(5)]
		4	0.302	1.109	0.195	0.541	1.230	1.139	0.12
		6	0.290	1.688	0.202	-0.83	1.220	1.055	0.03
^{148}Ce	G	0	0.0	0.0(-264.103)	0.343	0.0	1.026	0.967	-
					[0.246(10)]		[1.102]	[0.795]	
		2	0.100	0.117	0.337	0.080	1.026	0.992	0.26
				[0.159]					[+0.37(6)]
		4	0.118	0.534	0.380	0.059	0.940	0.692	0.23
		6	0.154	0.856	0.382	0.101	0.918	0.608	0.20
^{146}Ce	F	0	0.0	0.0(-253.008)	0.168	0.0	1.118	1.329	-
					[0.174(12)]		[1.178]	[1.056]	
		2	0.276	0.402	0.196	1.536	1.015	1.236	0.45
				[0.258]					[+0.24(5)]
		4	0.294	1.044	0.211	0.968	0.972	1.151	0.27
		6	0.279	1.552	0.224	-0.02	0.953	1.074	0.16
^{148}Ce	F	0	0.0	0.0(-264.753)	0.337	0.0	0.842	1.022	-
					[0.246(10)]		[1.102]	[0.795]	
		2	0.091	0.117	0.341	0.076	0.822	0.983	0.33
				[0.159]					[+0.37(6)]
		4	0.139	0.354	0.349	0.171	0.781	0.895	0.34
		6	0.164	0.663	0.356	0.239	0.726	0.795	0.36

[a,b]Two different minima obtained depending on the initial choices of β_2 and γ.

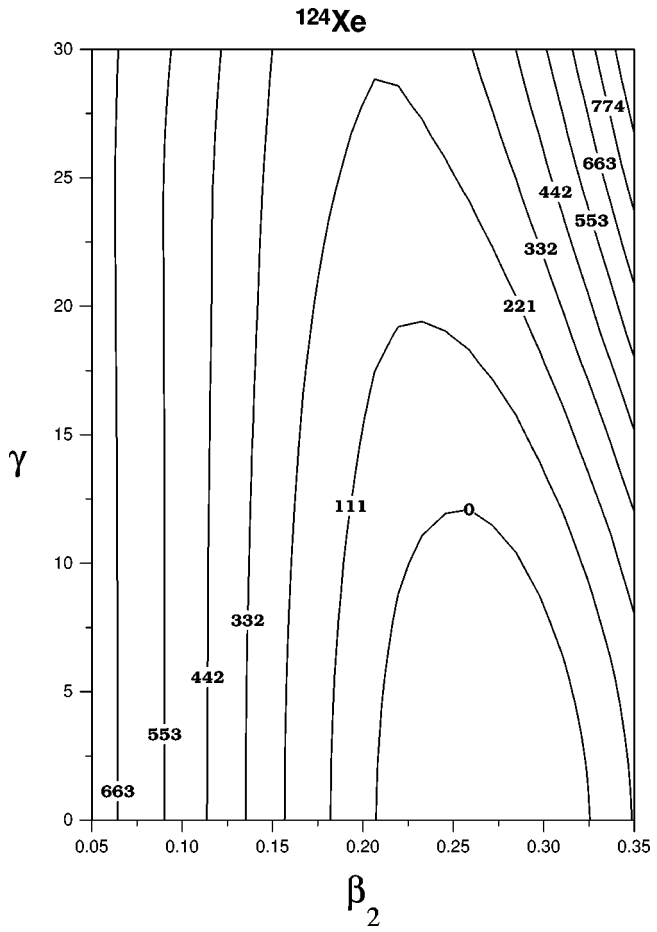

FIG. 1. Energy contour plot in the β_2-γ space for ^{124}Xe. The energy (in keV), relative to the minimum, corresponding to each contour line is marked in the figure.

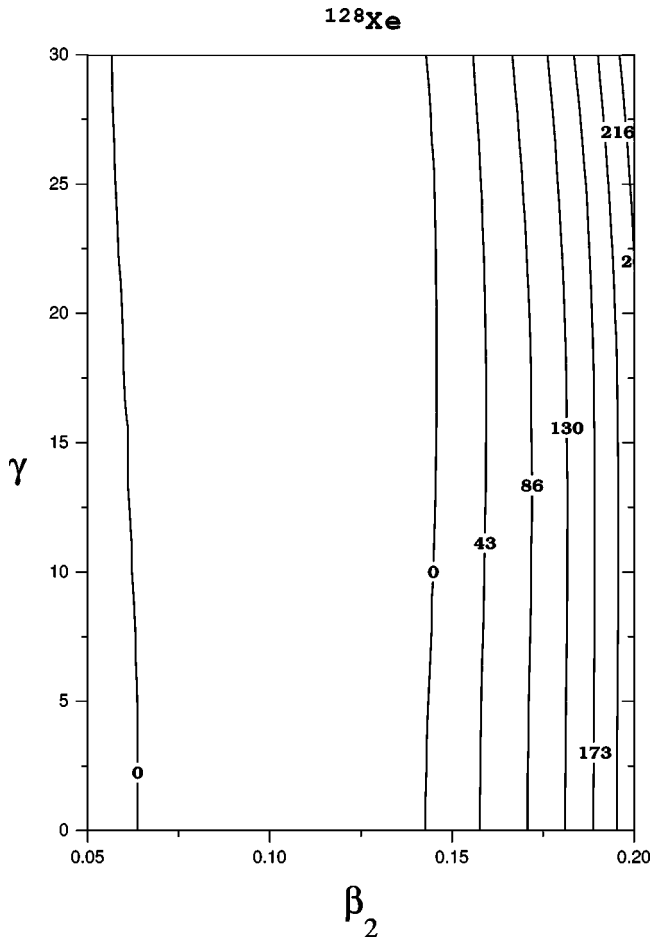

FIG. 2. Energy contour plot in the β_2-γ space for ^{128}Xe. The energy (in keV), relative to the minimum, corresponding to each contour line is marked in the figure.

The energy contour plot of ^{128}Xe thus explains the extreme sensitivity of the results (specially the γ values) to the limits of iterations.

For the $N=76$, 78 Xe isotopes, i.e., ^{130,132}Xe, this set of parameters fail completely. The ground state deformations come out to be almost zero. For $N=76$, the 2^+ state deformation increases to 0.10, showing a large triaxiality ($\gamma \simeq 22°$), and a strong neutron alignment, showing a negative g factor. The $N=78$ isotope loses collectivity and comes closer to complete sphericity. These nuclei have only 2 or 3 neutrons less than a complete shell closure. Moreover, xenon ($Z=54$) nuclei have only 4 valence protons above the $Z=50$ shell closure, although the number of unoccupied states are quite large for them.

The parameter set chosen reproduces the pairing gaps reasonably for ^{124}Xe, with slightly smaller value for Δ_p. For ^{122}Xe experimental pair gaps are somewhat larger than the theoretical values. We have compared the values in Table III. For heavier masses, the calculated proton pairing gaps are consistently larger than the theoretical values. The ^{130}Xe isotope shows an extremely strong neutron alignment at $I=2^+$, unlike the experimental situation. To retard the neutron alignment for this isotope and to see its effect on the calculated spectra, we could have either reduced the G_p value or increased the value of G_n. To have an idea about the effect of such a retardation we have only reduced G_p to 26.0 (Table III). The proton pairing gap decreases as expected, but the deformation also decreases. So there is no overall improvement in the results.

Keeping the potential parameter set fixed, we then changed the set of spherical single particle energies (s.p.e.) to those suggested by Nilsson [16]. But this set of s.p.e. does not reproduce the increasing trend of g factors from ^{124}Xe to ^{126}Xe (Table III). We have not varied the parameter sets (G_p, G_n, etc.) to have a better fit with the Nilsson set of single particle energies. Rather we decided to stick to the Zhang set of single particle energies, which is more realistic for predicting the bandhead energies in this mass region.

D. $^{130-136,\,142-146}_{56}Ba_{74-80,\,86-90}$

The results are shown in Table III. The g-factor data, neutron pairing gap for ^{130}Ba is reproduced reasonably, though the values of deformation (excitation energy) are smaller (larger) than experimental values. The proton pairing gap is larger than that obtained from the odd-even mass difference. For $N=76$ ^{132}Ba nucleus, the g-factor value is abnormally low, deformation is smaller than the experimental value, the proton pairing gap is quite big compared to the odd-even (o-e) mass difference. For ^{134,136}Ba the neutron numbers are 78 and 80, respectively, very close to the shell closure at $N=82$. As a result the deformation comes out to

be almost zero at the ground state and the model fails to predict the properties of higher spin states by iteration. So we have excluded these two nuclei from our calculations. The properties of second set of Ba nuclei with $A=142-146$ and $N=86-90$ have been calculated with the neutron valence shells, $N=5$ and 6 with $N_{\rm core}=70$. The initial set of calculations with the standard set of parameters used so far yields energy values largely off from the experimental numbers. The deformation and pairing gaps are also not reproduced properly. The g-factor values on the other hand for the $A=144,146$ nuclei are reproduced quite reasonably.

The general trend in all these Ba nuclei indicate that the parameter values need some modifications. The observations can be summarized as follows.

The proton pairing gaps are consistently larger than the experimental o-e mass differences except for ^{144}Ba and for ^{146}Ba, for which the o-e mass difference is not calculated due to lack of experimental data.

The deformation values are smaller than the experimental β_2 values for the lower masses but exceeds them for higher masses ($A=144,146$).

The g-factor values are smaller than the experimental data for all the isotopes except $A=144$.

The neutron pairing gaps are also larger than those deduced from the o-e mass differences.

Thus both the proton and neutron pairing strengths need adjustments. The proton pairing strength was adjusted first. It was reduced to have better agreement with the pairing gap and g-factor data. Reduced proton pairing strength is expected to lead to an increased g-factor value because of better proton alignment. So the next set of calculation is performed with G_p reduced to 26 and keeping other parameters unaltered. The g factor of the 10^+ state of ^{132}Ba, calculated with this parameter set (set B, Table I) comes out to be -0.18, whereas the measured value is $-0.159(5)$ [11]. Another attempt was made with G_p equal to 26 and G_n equal to 22 (set D, Table I). At least for ^{130}Ba, this set seems to be the best.

The calculations for higher mass isotopes ($^{142-146}$Ba) have been repeated with $G_p=26$, $G_n=24$ and $\chi_2=75$ (set E, Table I) and the combination has also been repeated with the Nilsson set of spherical single particle energies (set F, Table I). The results are shown in Table III.

E. $^{126,\,132,134,\,146,148}_{58}Ce_{68,74,76,88,90}$

The results are shown in Table IV. The g-factor data, proton, neutron pairing gaps, and deformations are shown there for different sets of parameter values for 0^+ to 6^+ state of these isotopes. The ^{126}Ce nucleus shows a proton alignment which agrees with the experimental findings as already discussed. The results are self-explanatory from Table IV. For the ^{134}Ce isotope, the final value of nonaxiality shows a strong dependence (Table IV) on the choice of input value of γ deformation. The energy remains more or less constant over a large range of γ values for the 0^+ state. Two such results for the 0^+ state have been mentioned in Table IV. For the 2^+ also, the minimum energy configuration with respect to the γ degree of freedom differs drastically (as shown by two different minimum energy configurations for 2^+ state in Table IV, where γ values are $\approx 2°$ and 20°) depending on the initial conditions. These two configurations differ by only $\simeq$ 100 keV. As a result the γ value at the final minimum obtained for each spin state is a sensitive function of the input γ value. This feature has been clearly expressed in the total energy contours drawn for ground state ($\beta_4=0.0$ in Fig. 3). The contours are parallel to the γ axis, and thus are independent of the γ value. So there is no way of predicting the best value of γ.

To see the effect of hexadecapole degrees of freedom (β_4 deformation), we started with the full Hamiltonian (4) with χ_4 value as mentioned before. The other parameters are the same as set C of Table I. The input values of β_2, γ and pairing gaps were chosen corresponding to the earlier minimum ($E_{\rm min}=-224.606$ MeV) without the hexadecapole term. They are

$$\beta_2=0.1293, \quad \gamma=0.0, \quad \Delta_p=1.69513 \text{ MeV},$$

$$\text{and} \quad \Delta_n=1.26405 \quad \text{MeV}.$$

The self-consistently calculated values of the potential parameters corresponding to the new minimum with a hexadecapole term in the Hamiltonian are

$$\beta_2=0.1299, \quad \gamma=0.0, \quad \Delta_p=1.69599 \quad \text{MeV},$$

$$\text{and} \quad \Delta_n=1.25629 \quad \text{MeV},$$

$$\text{with} \quad \beta_4=-0.005.$$

The energy corresponding to this minimum is -224.611 MeV. So the gain in the total binding energy is extremely small. The sign of the self-consistent value of β_4 determined agrees with the sign predicted by Möller *et al.* [21] ($\beta_4=-0.023$). The magnitude does not agree. The χ_4 value may have to be increased to have a good agreement.

It was pointed out by Ragnarsson *et al.* [22] that the effect of the β_4 term is to favor the prolate shape compared to the oblate one. We therefore introduced constant β_4 values in the Hamiltonian to see its effect on the energy surfaces. The variation with the change in the absolute value and the sign of β_4 is shown in Fig. 3. In the figure with $\beta_4=0.03$, the energy contours have already started to show a small deviation from the flat contours of the figure where $\beta_4=0.0$. With an increase in β_4 value ($=0.09$) a definite prolate minimum has developed around $\beta_2\simeq 0.10$. Finally, for $\beta_4=-0.09$, the change in the sign of β_4 has resulted in a γ soft minimum about $\beta_2\simeq 0.13$.

IV. DISCUSSIONS

The equilibrium deformation for the ground state in Te, Xe, Ba, and Ce nuclei has been systematically studied in this work. Some of our important observations may be summarized as follows: In each isotonic chain the quadrupole deformation increases with increasing Z. On the other hand, in each isotopic chain, the deformation (β_2) decreases with increasing neutron number. The triaxiality (γ) increases with increasing neutron number showing a change of shape from prolate to triaxial to oblate. Both β_2 and γ eventually reduce to zero which correspond to a spherical shape near the $N=82$ shell closure (Tables III and IV).

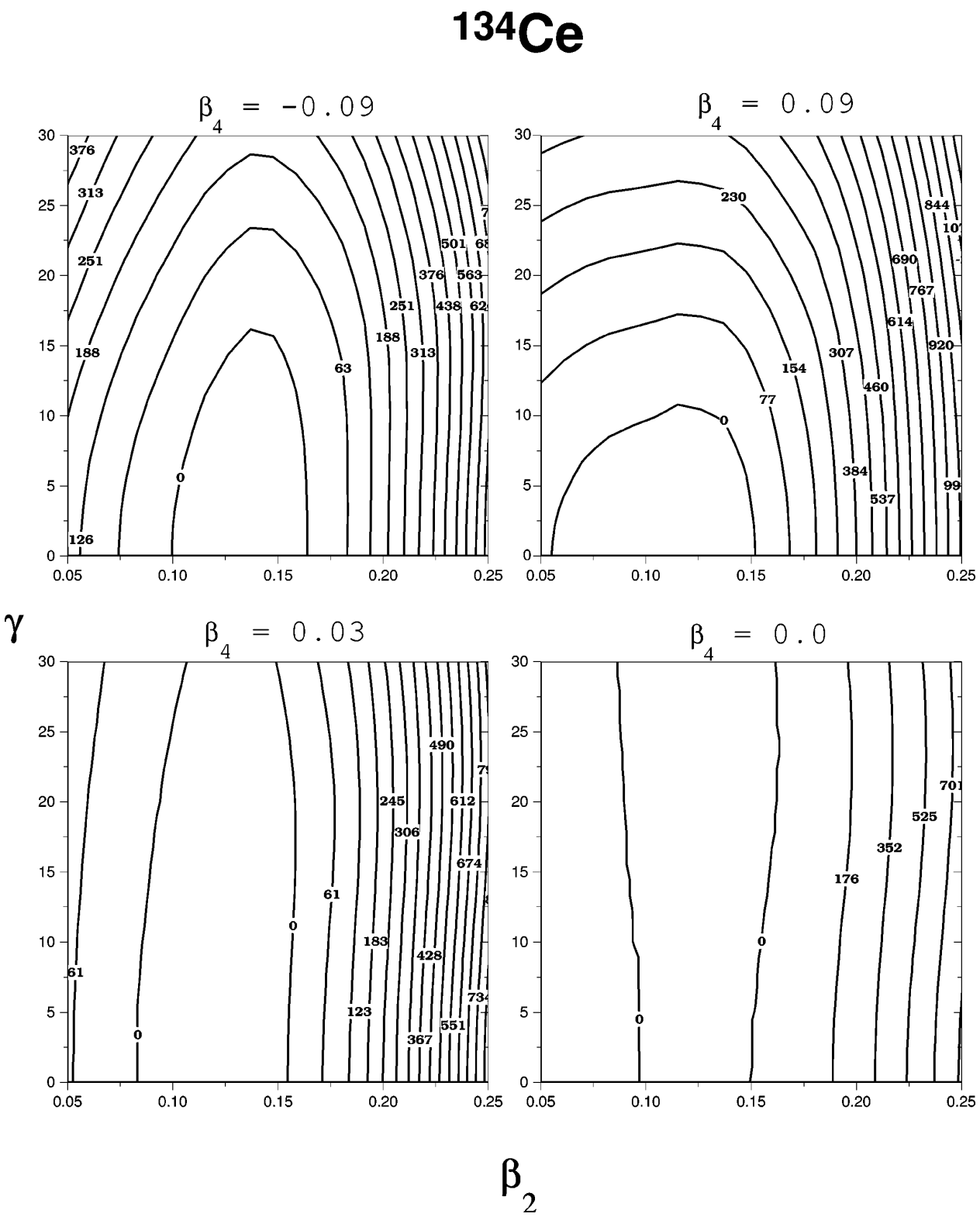

FIG. 3. Energy contour plots in the β_2-γ space for ^{134}Ce with and without hexadecapole deformation. The values of β_4 chosen are marked in the figures. The energy (in keV), relative to the minimum, corresponding to each contour line is also marked.

The increase in deformation in isotonic chains can be related to the increasing proton occupation of the deformation driving low Ω $\pi h_{11/2}$ orbitals. Similarly with increasing neutron number, more and more high-Ω $\nu h_{11/2}$ orbitals will be occupied leading to smaller and smaller deformation. It is also noticed that in all the isotopes, the lowest ($\nu h_{11/2}$) configuration becomes oblate only for $N=76$.

V. CONCLUSION

On the basis of a comparative study of the results of the present work with those of earlier theoretical and experimental investigations in this region as well as in other mass regions, the following conclusions may be drawn.

A reasonable fit to the ground state properties and to the

observed g-I variations in this transitional region can be obtained in a simple version of the CHFB calculation using proper values of the monopole pairing and the quadrupole-quadrupole interaction strength parameters along with the spherical single particle energies prescribed by Zhang *et al.*

A weak hexadecapole term (resulting in a small value of β_4) introduced in the calculation has been seen to reduce the gamma softness of the nuclei in this mass region. This extra term introduces a very small increase in the depth of the energy minimum. So theoretically it is very difficult to predict whether these nuclei have hexadecapole deformation or they are soft towards triaxial deformation.

The present work also suggests that the following theoretical and experimental investigations would lead to a better understanding of the nuclear structure of this mass region.

Experimental data on the g factors of high spin states are not available in almost all the nuclei in this mass region. The g-factor data are essential to properly understand and investigate the intricacies of nuclear structure in a particular mass region.

More experimental information about the hexadecapole deformation as well as the triaxiality of these nuclei are essential to understand these nuclei more deeply. This information will help to actually decide whether the quadrupole-quadrupole interaction term in the Hamiltonian is adequate for the description of these nuclei.

The nuclei with neutron numbers 78–82 need some special attention. Their structure is almost spherical. They have only noncollective shell model states in their low excitation spectra. This type of structure needs some special effort to be explained by this version of the CHFB model. Study of such nuclei using the CHFB formalism will be a very interesting problem.

ACKNOWLEDGMENT

We would like to thank Professor A. Ansari for many helpful discussions.

[1] J.R. Hughes, D.B. Fossan, D.R. LaFosse, Y. Liang, P. Vaska, and M.P. Waring, Phys. Rev. C **44**, 2390 (1991); R. Goswami, B. Sethi, P. Banerjee, and R.K. Chattopadhyay, *ibid.* **47**, 1013 (1993); Y. Liang, D.B. Fossan, J.R. Hughes, D.R. LaFosse, T. Lauritsen, R. Ma, E.S. Paul, P. Vaska, M.P. Waring, and N. Xu, *ibid.* **45**, 1041 (1992).

[2] M. Saha Sarkar, A. Goswami, S. Bhattacharya, B. Dasmahapatra, P. Bhattacharya, P. Basu, M.L. Chatterjee, and S. Sen, J. Phys. G **23**, 169 (1997).

[3] M. Saha Sarkar, A. Goswami, S. Bhattacharya, B. Dasmahapatra, P. Bhattacharya, P. Basu, M.L. Chatterjee, and S. Sen (unpublished).

[4] R. Wyss *et al.*, Nucl. Phys. **A505**, 337 (1989).

[5] Y.S. Chen, S. Frauendorf, and G.A. Leander, Phys. Rev. C **28**, 2437 (1983).

[6] G. Andersson *et al.*, Nucl. Phys. **A268**, 205 (1976).

[7] K. Kumar and M. Baranger, Nucl. Phys. **A110**, 490 (1968); **A110**, 529 (1968); **A122**, 241 (1968).

[8] M. Diebel, A.N. Mantri, and U. Mosel, Nucl. Phys. **A345**, 72 (1980); Phys. Scr. **24**, 331 (1981); A. Ansari, E. Wüst, and K. Mühlhans, Nucl. Phys. **A415**, 215 (1984); K. Sugawara-Tanabe and K. Tanabe, Phys. Lett. B **207**, 243 (1988).

[9] M. Saha and S. Sen, Phys. Lett. B **252**, 181 (1990).

[10] M. Saha and S. Sen, Nucl. Phys. **A552**, 37 (1993).

[11] Pragya Das, R.G. Pillay, V.V. Krishnamurthy, S.N. Mishra, and S.H. Devare, Phys. Rev. C **53**, 1009 (1996).

[12] A. Ansari, Phys. Rev. C **38**, 323 (1988).

[13] A.L. Goodman, Nucl. Phys. **A230**, 466 (1974); **A265**, 113 (1976); A. Faessler, K.R. Sandhya Devi, F. Grümmer, K.W. Schmid, and R.R. Hilton, *ibid.* **A256**, 106 (1976); A. Ansari and S.C.K. Nair, *ibid.* **A283**, 326 (1977).

[14] A. Ansari, Phys. Rev. C **33**, 321 (1986).

[15] J. Zhang, N. Xu, D.B. Fossan, Y. Liang, R. Ma, and E.S. Paul, Phys. Rev. C **39**, 714 (1989).

[16] S.G. Nilsson, C.F. Tsang, A. Sobiczewski, Z. Szymanski, S. Wycech, C. Gustafson, I.L. Lamm, P. Moller, and B. Nilsson, Nucl. Phys. **A131**, 1 (1969).

[17] P. Raghavan, At. Data Nucl. Data Tables **42**, 189 (1989).

[18] A. Faessler, M. Ploszajczak and K.W. Schimd, in *Progress in Particle and Nuclear Physics*, edited by D. Wilkinson (Pergamon Press, Oxford, 1981), Vol. 5, p. 79.

[19] S. Raman, C.H. Malarkey, W.T. Milner, C.W. Nestor, Jr., and P.H. Stelson, At. Data Nucl. Data Tables **36**, 1 (1987).

[20] M. Sakai, At. Data Nucl. Data Tables **31**, 399 (1984).

[21] P. Möller, J.R. Nix, W.D. Myers, and W.J. Swiatecki, At. Data Nucl. Data Tables **59**, 185 (1995).

[22] I. Ragnarsson, A. Sobiczewski, R.K. Sheline, S.E. Larsson, and B. Nerlo-Pomorska, Nucl. Phys. **A233**, 329 (1974); A. Ansari, Phys. Rev. C **38**, 953 (1988).

[23] J. Hattula, S. Juutinen, M. Jaaskelainen, T. Lonnroth, A. Pakkanen, M. Piiparinen, and G. Sletten, J. Phys. G **13**, 57 (1987).

[24] W. Gast, U. Kaup, H. Hanewinkel, R. Reinhardt, K. Schiffer, K.P. Schmittgen, K.O. Zell, J. Wrzensinski, A. Gelberg, and P. V. Brentano, Z. Phys. A **318**, 123 (1984).

[25] R. Moscrop, M. Campbell, W. Gelletly, L. Goettig, C.J. Lister, B.J. Varley, and H.G. Price, Nucl. Phys. **A481**, 559 (1988).